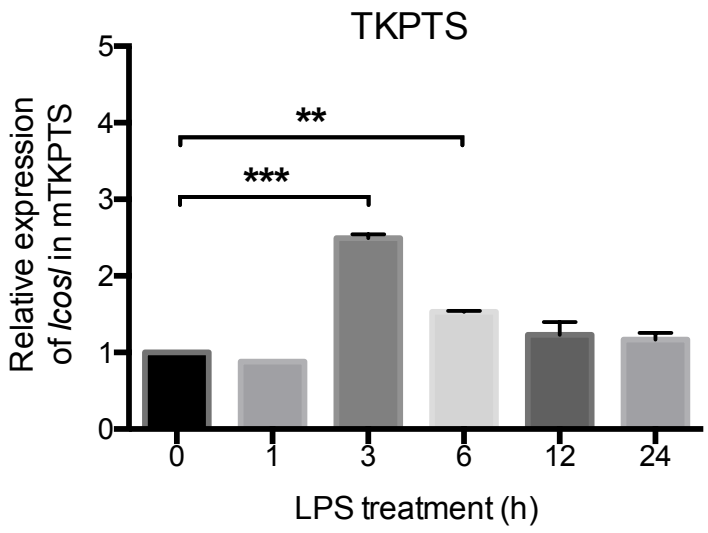

Supplemental Figure 1.

Expression levels of *Icosl* are increased by LPS in mouse kidney proximal tubule cell line (TKPTS). Relative mRNA expression measured by quantitative PCR targeting *Icosl* in mouse TKPTS cells that were treated with 50 μg/ml LPS for 1, 3, 6, 12 and 24 hours. QPCR analysis of *Icosl* mRNA was normalized to the expression of *Gapdh* and presented relative to *Icosl* expression levels in untreated cells. n=3 biologically independent samples. Data are mean±SD; $^{**}P<0.01$, $^{***}P<0.001$; One-way ANOVA with Tukey's multiple comparison test.

A

1. **B7.1**; NP_005182.1 T-lymphocyte activation antigen CD80 precursor, B7.1
2. **B7.2**; NP_787058.4 T-lymphocyte activation antigen CD86 isoform 1 precursor, B7.2
3. **ICOSL**; NP_056074.1 **ICOS ligand** isoform a precursor
4. **PDL-1**; NP_054862.1 programmed cell death 1 ligand 1 isoform a precursor

```
1. NP_005182.1      MGHTRRQGTSPSKCPY----LNFFQLLVLAGLSHFCSGVIHVTKEVKEVATLSCGHNV-S   55
2. NP_787058.4      ---------MDPQCTMGLSNILFVMAFLLSGA-----APLKIQAYFNETADLPCQFANSQ   46
3. NP_056074.1      -------------MRLGSPGLLFLLFSSLRA----DTQEKEVRAMVGSDVELSCACPEGS   43
4. NP_054862.1      -------------MRIF-AVFIFMTYWHLLNAFTVTVPKDLYVVEYGSNMTIECKFPVEK   46
                                          : *.    *                  .   : *     .

1. NP_005182.1      VEELAQTRIYWQKEKKMV-LTMMSGDM----NIWPEYKNRTIFDI----TNNLSIVILAL   106
2. NP_787058.4      NQSLSELVVFWQDQENLV-LNEVYLGKEKFDSVHSKYMGRTSFDS----D-SWTLRLHNL   100
3. NP_056074.1      RFDLNDVYVYWQTSESKTVVTYHIPQNSSLENVDSRYRNRALMSPAGMLRGDFSLRLFNV   103
4. NP_054862.1      QLDLAALIVYWEMEDKNI-IQ-FVHGEEDLKVQHSSYRQRARLLKDQLSLGNAALQITDV   104
                      .*    ::*: ...   :                *  *: :        . :: :  :

1. NP_005182.1      RPSDEGTYECVVLKYEKDAFKREHLAEVTLSVKADFPTPSISDFEIPT-SNIRRIICSTS   165
2. NP_787058.4      QIKDKGLYQCIIHHKKPTGMIRIHQMNSELSVLANFSQPEIVPISNITENVYINLTCSSI   160
3. NP_056074.1      TPQDEQKFHCLVLSQ-SLGFQEVLSVEVTLHVAANFSVPVVSAPHSPS-QDELTFTCTSI   161
4. NP_054862.1      KLQDAGVYRCMISYG-GADYKRIT-----VKVNAPYNKINQRILVVDPVTSEHELTCQ-A   157
                      .*   :.*::         .       : * * :                  : *

1. NP_005182.1      GGFPEPHLSWLENGEELNAI----NTTVSQDPETELYAVSSKLDFNM---TTNHSFMCLI   218
2. NP_787058.4      HGYPEPKKMSVLLRTKNSTIEYDGIMQKSQDNVTELYDVSISLSVSFPDVTSNMTIFCIL   220
3. NP_056074.1      NGYPRPNVYWINKTDN-SLLDQALQNDTVFLNMRGLYDVVSVLRIAR---TPSVNIGCCI   217
4. NP_054862.1      EGYPKAEVIWTSSDHQVL---SGKTTTTNSKREEKLFNVTSTLRINT---TTNEIFYCTF   211
                     *:*. .        :                  *: *   * .     * .  : * :

1. NP_005182.1      KYGHLRVNQ-----T------FNWNTTKQEHFPDNLLPSWAITLISVNGIFVICCLTYCF   267
2. NP_787058.4      ETDKTRLLS----SP------FSIELEDPQPPPD--HIPWITAV---LPTVIICVMVFCL   265
3. NP_056074.1      ENVLLQQNLTVGSQTGNDIGERDKITENPVSTGEKNAATWSILA-------VLCLLVVVA   270
4. NP_054862.1      RRLDPEENHTAE----------LVIPELPLAH-----PPNERTHLVILGAILLCLGV-AL   255
                    .    .                                                ::*  .

1. NP_005182.1      APRCRERRRNE---------RLRRESVRPV------------------------------   288
2. NP_787058.4      ILWKWKKKKRPRNSYKCGTNTMEREESEQTKKREKIHIPERSDEAQRVFKSSKTSSCDKS   325
3. NP_056074.1      VAIGWVCRDRCLQHSYAGAWAVSPETE-LTG-----HV----------------------   302
4. NP_054862.1      TFIFRLRKGRMMDVKKCGIQDTNSKKQS------DTHLEET-------------------   290
                           : .              :

1. NP_005182.1      ----          288
2. NP_787058.4      DTCF          329
3. NP_056074.1      ----          302
4. NP_054862.1      ----          290
```

B

Protein Accession No.	Organism	Gene
1. NP_056074.1	H.sapiens	*ICOSLG*
2. XP_006723963.1	H.sapiens	*LOC102723996*
3. XP_003319157.1	P.troglodytes	*ICOSLG*
4. XP_002803158.1	M.mulatta	*LOC722191*
5. XP_005639015.1	C.lupus	*ICOSLG*
6. XP_005202100.1	B.taurus	*ICOSLG*
7. NP_056605.1	M.musculus	*Icosl*
8. XP_006256322.1	R.norvegicus	*Icoslg*
9. NP_990415.1	G.gallus	*ICOSLG*

```
1. NP_056074.1      1   MRL-------------------------GSPGLLFLLFSSLRADTQEKEVRAMVGSDVELSCACPEGSRFDLNDVYVYWQTSES-----KTVVTYHIP--   68
2. XP_006723963.1   1   MRL-------------------------GSPGLLFLLFSSLRADTQEKEVRAMVGSDVELSCACPEGSRFDLNDVYVYWQTSES-----KTVVTYHIP--   68
3. XP_003319157.1   1   MRL-------------------------GSPGLLFLLFSSLRADTQEKEVRAMVGSDVELSCACPEGSRFDLNDVYVYWQTSES-----KTVVTYHIP--   68
4. XP_002803158.1   1   MRL-------------------------GSPGLLLLLFSSLRADTQEKEVRAMVGSDVELSCACPEGSRFDLNDVYVYWQTSES-----KTVVTYHIP--   68
5. XP_005639015.1   1   MWL-------------------------RCPGVLLLLLGTLQANTQEQEVKALVGSSVELRCVFPERHTFDLDDLYVYWQISVVGQ---PKTVTYYLS--   70
6. XP_005202100.1   1   MRP-------------------------RSPGLFLLLLWGLQAESQE-EVRAMVGSDVQLRCIYPEKNSFDLNDLYVYWQISMAGKGNVDSVVTYHLS--   72
7. NP_056605.1      1   MQLKCPCFVSLGTRQPVWKKLHVSSGFFSGLGLFLLLLSSLCAASAETEVGAMVGSNVVLSCIDPHRRHFNLSGLYVYWQI-ENP----EVSVTYYLP--   93
8. XP_006256322.1   1   MQL---------------------NRFFSGPGLFLLLFCSLCVEAEVKEVNAMVGSDVELRCVYPRRSHFSLDDLYVYWQIVDEA----KTVVTYYLPSA   75
9. NP_990415.1      1   MKR-------------------------LGYGFLLLFLHILRAVTALEKIISKPGDNATLSCIYANRG-FDLDSLRVYWQIDGVEGSKSCSVVHALIS--   72

1. NP_056074.1     26  RAMVGSDVELSCACPEGSRFDLNDVYVYWQTSES-----KTVVTYHIP--QNSSLENVDSRYRNRALMSPAGMLRGDFSLRLFNVTPQDEQKFHCLVL-S   117
2. XP_006723963.1  26  RAMVGSDVELSCACPEGSRFDLNDVYVYWQTSES-----KTVVTYHIP--QNSSLENVDSRYRNRALMSPAGMLRGDFSLRLFNVTPQDEQKFHCLVL-S   117
3. XP_003319157.1  26  RAMVGSDVELSCACPEGSRFDLNDVYVYWQTSES-----KTVVTYHIP--QNSSLENVDSRYRNRALMSPAGMRRGDFSLRLFNVTPQDEQKFHCLVL-S   117
4. XP_002803158.1  26  RAMVGSDVELSCACPEGSRFDLNDVYVYWQTSES-----KTVVTYHIP--QNSSLDNVDSHYRNRALMSPAGMQRGDFSLRLFNVTPQDEQKFHCLVL-S   117
5. XP_005639015.1  26  KALVGSSVELRCVFPERHTFDLDDLYVYWQISVVGQ---PKTVTYYLS--GNSSTGQEDDRYRDRARLSPESMQRGDFSLHLYNITPYDEQKFNCLVF-R   119
6. XP_005202100.1  25  RAMVGSDVQLRCIYPEKNSFDLNDLYVYWQISMAGKGNVDSVVTYHLS--GNSSASHGDNHYKDRARLSLDSMKQGDFSLHLRNVTPQDEQKFNCLVF-R   121
7. NP_056605.1     51  GAMVGSNVVLSCIDPHRRHFNLSGLYVYWQI-ENP----EVSVTYYLP--YKSPGINVDSSYKNRGHLSLDSMKQGNFSLYLKNVTPQDTQEFTCRVFMN   143
8. XP_006256322.1  30  NAMVGSDVELRCVYPRRSHFSLDDLYVYWQIVDEA----KTVVTYYLPSANESSTIHVSNSYKNRAHLSPDLMKEGDFSLHLQNVTPQDTQEFKCLVF-R   124
9. NP_990415.1     26  ISKPGDNATLSCIYANRG-FDLDSLRVYWQIDGVEGSKSCSVVHALIS--GQDNESQQCSQFKNRTQLLWDKLGDGDFSLLLYNVRQSDEHTYKCVVM--   120

1. NP_056074.1    118  QSLGFQEVL-SVEVTLHVAANFSVPVVSAP--HSPSQD-ELTFTCTSINGYPRPNVYWINKTDNSLLDQALQNDTVFLNMRGLYDVVSVLRIARTPSVNI   213
2. XP_006723963.1 118  QSLGFQEVL-SVEVTLHVAANFSVPVVSAP--HSPSQD-ELTFTCTSINGYPRPNVYWINKTDNSLLDQALQNDTVFLNMRGLYDVVSVLRIARTPSVNI   213
3. XP_003319157.1 118  QSLGFQEVL-SIEVTLHVAANFSVPVVSTP--HSPSQD-ELTFTCTSINGYPRPNVYWINKTDNSLLDQALQNDTVFLNTRGLYDVVSVLRIARTPSVNI   213
4. XP_002803158.1 118  QSLGFQEVL-SVVVTLHVAANFSVPVVSTP--HNPSQD-KLTFTCTSINGYPRPNVYWINKTDNSLLDQALQNDTVFLNTRGLYDVVSVLRIARTPSLNI   213
5. XP_005639015.1 120  KSLELKKIL-DVEVTLHVAANYSMPVVSAP--SDPSKDRELTFTCTSVNGYPRPNVYWINKTDNSVLDGGLQNHTVSVNAQGLYDVVSVLRVPWAPSINV   216
6. XP_005202100.1 122  KSLELKKIL-EVAVTLHVAANYSMPVVSG-----PSQDEELTFTCTSTNGYPRPNVYWINKTDNSVLDSALQNNTVSLNARGLYDVVSVLRIGRTPHVNV   215
7. NP_056605.1    144  TATELVKIL-EEVVRLRVAANFSTPVISTS--DSSNPGQERTYTCMSKNGYPEPNLYWINTTDNSLIDTALQNNTVYLNKLGLYDVISTLRLPWTSRGDV   240
8. XP_006256322.1 125  MSTVLGKAL-EEVVRLRVAANFSTPVISTS--GSSDPGQERTFTCMSKNGYPEPNLYWINRTDNTLIDETLQNNTVYLNELGLYDVVSTLRIPWTPHVDV   221
9. NP_990415.1    121  QTIEYTRVIHQEQVVLSLAASYSQPILSGPIRNSYSTGEEVTFSCRSDNGYPEPNVYWINRTDNTRLSQS--DFNITQHPDGTYSVLSTLKVNATSDMQL   218

1. NP_056074.1    214  GCCIENVLLQQNLTVGSQTGNDIGERDKITENPV--STGEKNAATWSILAVLCLLVVVAVAIG-WVCRDRCL----------------------------   282
2. XP_006723963.1 214  GCCIENVLLQQNLTVGSQTGNDIGERDKITENPV--STGEKNAATWSILAVLCLLVVVAVAIG-WVCRDRCL----------------------------   282
3. XP_003319157.1 214  GCCIENVLLQQNLTVGSQTGNNIGERDKITENPV--STGEKNAATWSILAVLCLLVVVAVAIG-WVCRDRCL----------------------------   282
4. XP_002803158.1 214  GCCIENVLLRQNLTVGSQTGNNIGERDKITENPV--STREKTEVTWSVLAVLCLLVAVAVAIG-WVCRDRWL----------------------------   282
5. XP_005639015.1 217  GCCIENVLLHQNLTNR-PAEPIPGTEPGNTGSHRD-VHRRDHGAVLSAVAVLLVLALVLGAVG-CVCRSRCPRTDPCRLRLKRTRRLGRGQGFCEMPPGG   313
6. XP_005202100.1 216  GCCIENVLLHQNLTSG-QTETFTGTKDSITEDPVDGSPSGKHQQVFSVLAVLAVIVLLALATG-WLCRSRCP----------------------------   285
7. NP_056605.1    241  LCCVENVALHQNITSISQAESFTGN-N--TKNPQE-THNNELKVLVPVLAVLAAAAFVSFII--YR-RTR-P----------------------------   304
8. XP_006256322.1 222  ICCVENVALHQNITSISRADSFTGSMN--TERPQE-IHREATKVLFYVLAALLAVVVVIFIIVLYRCRRR-P----------------------------   289
9. NP_990415.1    219  ECFIENKVLQENTSANYTEEMQNNGSS--TGSHKDAAKGGQGAQAAAVVSVVILMAFLTVLIC-WLWRRRSF----------------------------   287

1. NP_056074.1    283  ------------QHSYAGAWA--------------------------VSPETELTGHV-------------------------------------------   302
2. XP_006723963.1 283  ------------QHSYAGAWA--------------------------VSPETELTGHV-------------------------------------------   302
3. XP_003319157.1 283  ------------QHSYAGAWA--------------------------VSPETELTGHV-------------------------------------------   302
4. XP_002803158.1 283  ------------RRSYAGVWA--------------------------VRPEPELAGEFAMGKQVQALAPTPTGCSEQVQALAPTPTGCSQQVQALAPTP   343
5. XP_005639015.1 314  TADGSLRIDPGRPGGQGGPAAPVGAVKKGASWPRDLSDLEGTRRIVLDARASVPAAAPILG-------------------------------------   374
6. XP_005202100.1 286  ------------PKSQTGAQV-------------------------ARPKLALAEHV-------------------------------------------   305
7. NP_056605.1    305  ------------HRSYTGPKT-------------------------VQLELTDHA-------------------------------------------   322
8. XP_006256322.1 290  ------------CQSYTGPRA-------------------------VQLELTGECTCGERPVG-------------------------------------   315
9. NP_990415.1         ------------------------------------------------QLVSYTAPV-------------------------------------------   296

1. NP_056074.1         ---------------------------------------------------------------------------------------------------
2. XP_006723963.1      ---------------------------------------------------------------------------------------------------
3. XP_003319157.1      ---------------------------------------------------------------------------------------------------
4. XP_002803158.1 344  TGCSEQVQALQVQALAPTPTGCSEQVQALVPSPHGVFRGGPGTCAHPYQDVRSRSRHCRLLSAAATPAALGRLPLSPEKTDVCLQNGKGCFMFLSLHFPS   443
5. XP_005639015.1      ---------------------------------------------------------------------------------------------------
6. XP_005202100.1      ---------------------------------------------------------------------------------------------------
7. NP_056605.1         ---------------------------------------------------------------------------------------------------
8. XP_006256322.1      ---------------------------------------------------------------------------------------------------
9. NP_990415.1         ---------------------------------------------------------------------------------------------------

1. NP_056074.1         ----------------
2. XP_006723963.1      ----------------
3. XP_003319157.1      ----------------
4. XP_002803158.1 444  KAMFDRSSPPRAWTGLP   460
5. XP_005639015.1      ----------------
6. XP_005202100.1      ----------------
7. NP_056605.1         ----------------
8. XP_006256322.1      ----------------
9. NP_990415.1         ----------------
```

Supplemental Figure 2.

Among B7 family members, only ICOSL gene contains an RGD motif which is highly conversed across different species. (**A**) Multiple sequence alignments of human B7 families; B7.1, B7.2, ICOSL and PDL-1 were aligned using the Clustal Omega server (1). (**B**) The ICOSL proteins used in this alignment were derived from HomoloGene database available at NCBI (http://www.ncbi.nlm.nih.gov/homologene/) and were 1. NP_056074.1 (H.sapiens), 2. XP_006723963.1 (H.sapiens), 3. XP_003319157.1 (P.troglodytes), 4. XP_002803158.1 (M.mulatta), 5. XP_005639015.1 (C.lupus), 6. XP_005202100.1 (B.taurus), 7. NP_056605.1 (M.musculus), 8. XP_006256322.1 (R.norvegicus), and 9. NP_990415.1 (G.gallus). In evolutionarily advanced vertebrates such as human (H.sapiens), chimpanzee (P.troglodytes), monkey (M.mulatta), and wolf (C.lupus), the RGD sequences are located in the IgV domain. In contrast, mouse (M.musculus) ICOSL has its RGD domain in the IgC domain. The RGD sequences are highlighted in red.

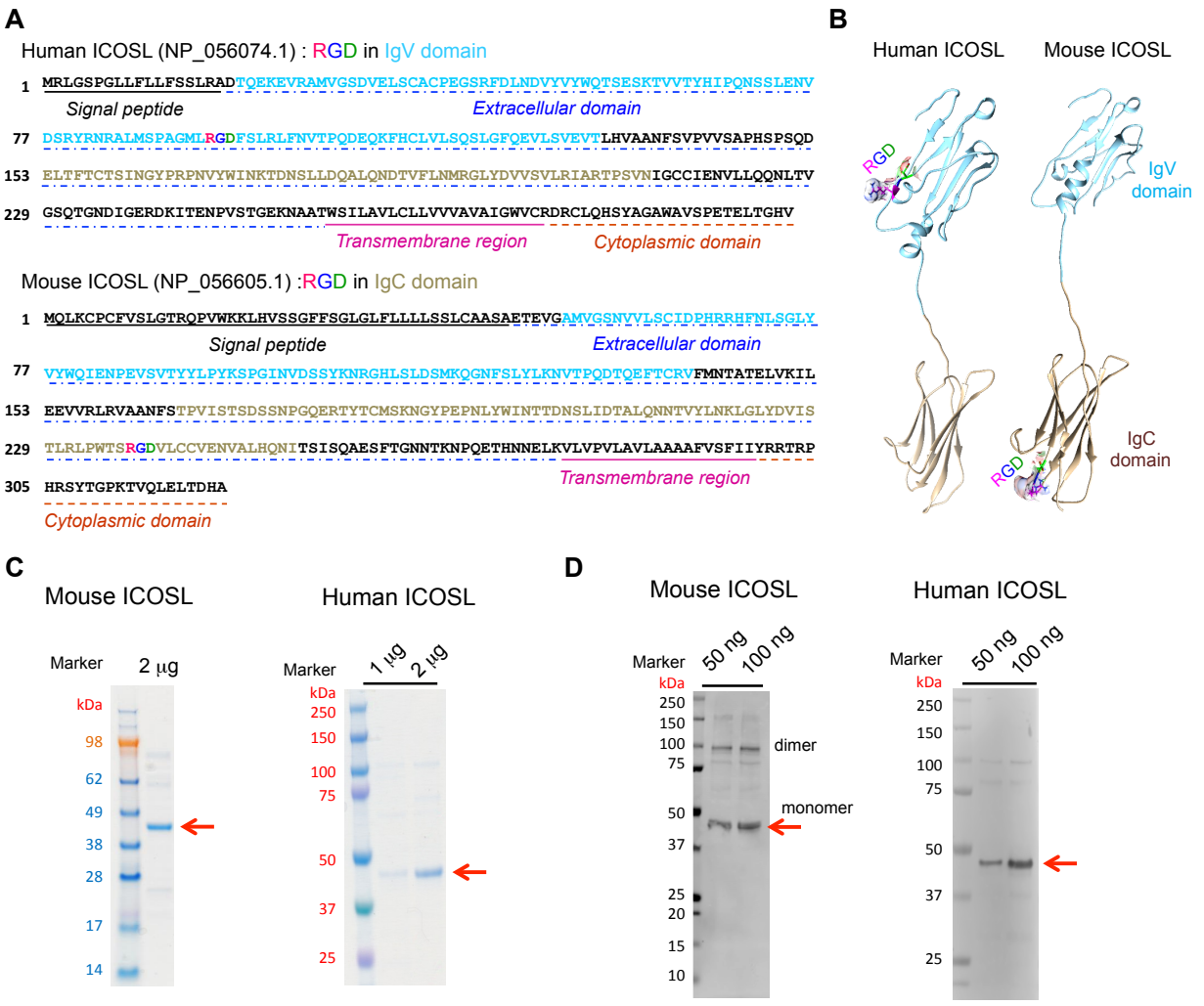

Supplemental Figure 3.

Both human and mouse ICOSL contain an RGD motif at an exposed loop region. (**A**) Sequence features of the RGD motif in human and mouse ICOSL domains. (**B**) Ribbon diagram of a three-dimensional model of the extracellular domains of human (left) and mouse ICOSL (right). (**C, D**) Quality and purity of the purified mouse and human recombinant ICOSL proteins were assessed using Coomassie Blue staining (**C**) and Western blotting (**D**). In SDS-PAGE gel staining, 1 or 2 µg of recombinant proteins were loaded in lanes 1 and 2, respectively. For Western-blotting, 50 and 100 ng of recombinant protein were separated on SDS-PAGE, transferred to a nitrocellulose membrane and incubated with rabbit anti-ICOSL antibody (MyBiosource, 1:500).

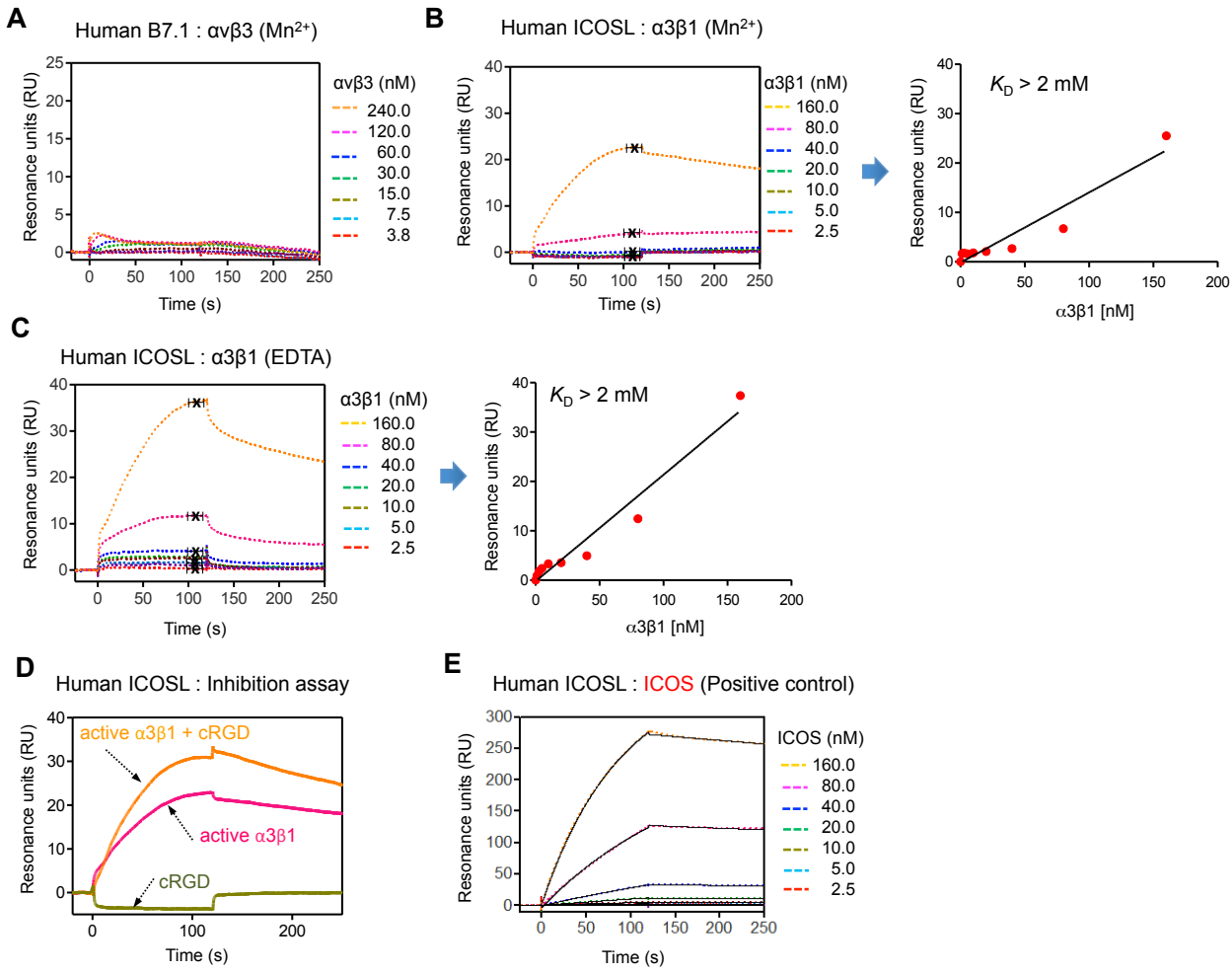

Supplemental Figure 4.

ICOSL shows no appreciable binding to α3β1 integrin. (**A**) SPR sensorgrams depicting interaction between immobilized human B7.1 and active (Mn^{2+}-induced) αvβ3 integrin at various concentrations (0-240 nM). (**B**, **C**) SPR sensorgrams depicting interaction between immobilized human ICOSL and active (**B**, 2 mM Mn^{2+} in binding buffer) or inactive (**C**, 3 μM EDTA in binding buffer) α3β1 integrin. On the *right-hand side* of each sensorgrams are the steady-state affinity fitting curves of α3β1 integrin (0-160 nM) binding to ICOSL. The K_D values determined for each of active or inactive α3β1 integrin were > 2 mM. (**D**) SPR illustrating the inhibition of α3β1 binding to ICOSL by the synthetic cRGD peptide. Injection of active α3β1 (160 nM) resulted in the binding signal for immobilized human ICOSL (pink curve). Preincubation with cRGDfv (30 μM) did not inhibit interaction with ICOSL, indicating that the RGD peptide did not compete with ICOSL for binding to α3β1 (orange curve). The cRGDfv alone was used as a

control (green curve). (**E**) SPR sensorgrams depicting interaction between immobilized human ICOSL and ICOS at various concentrations (0-160 nM). Kinetic constants (k_a, k_d) were derived from locally fitting the association and dissociation phases using a 1:1 Langmuir binding model (black fitting curves) and affinities were calculated as $K_D=k_d/k_a$. The average K_D values were determined from at least three independent experiments (**A**-**E**).

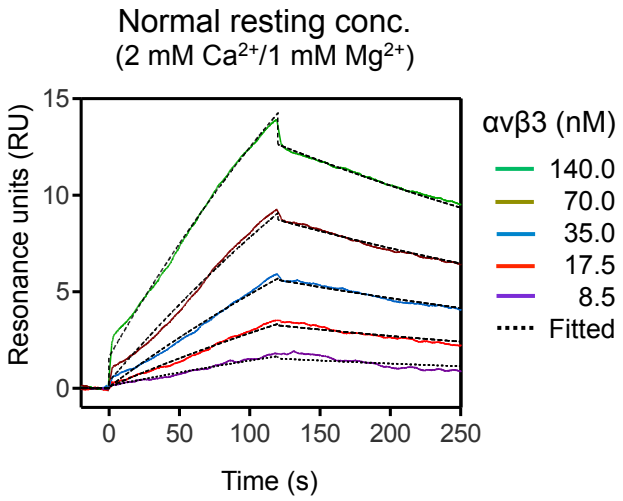

Concentrations of Ca^{2+} and Mg^{2+}	k_a (M^{-1} s^{-1})	k_d (s^{-1})	K_D (M)
2 mM, 1 mM	5.61 ± 0.97 x 10^3	2.18 ± 0.14 x 10^{-3}	400 ± 40 x 10^{-9}
0.2 mM, 0.1 mM (Figure 2H)	1.51 ± 0.39 x 10^5	3.26 ± 0.10 x 10^{-3}	21.3 ± 1.2 x 10^{-9}

Supplemental Figure 5.

The binding between ICOSL and αvβ3 integrin is inhibited under normal resting serum concentrations of Ca^{2+} and Mg^{2+} (2 mM and 1 mM, respectively). *Top:* Representative SPR sensorgram showing the binding between mICOSL protein and αvβ3 integrin under normal resting serum concentrations of Ca^{2+} and Mg^{2+} (2 mM and 1 mM, respectively). *Bottom:* Table summarizing the binding characteristics of ICOSL protein towards αvβ3 integrin under different concentrations of Ca^{2+} and Mg^{2+} (normal *vs* low). The average K_D values were determined from three independent experiments. Kinetic constants (k_a, k_d) were derived from locally fitting the association and dissociation phases using a 1:1 Langmuir binding model (black fitting curves) and affinities were calculated as $K_D=k_d/k_a$.

A

	Coupled protein	Cation	k_a (M^{-1} s^{-1})	k_d (s^{-1})	K_D (M)
I	αIIbβ3 integrin	2 mM Mn^{2+}	N.B	N.B	N.B
II	αvβ5 integrin		N.B	N.B	N.B
III	αvβ3 integrin		1.19 ± 0.09 x 10^{5}	1.99 ± 0.58 x 10^{-3}	16.2 ± 4.0 x 10^{-9}

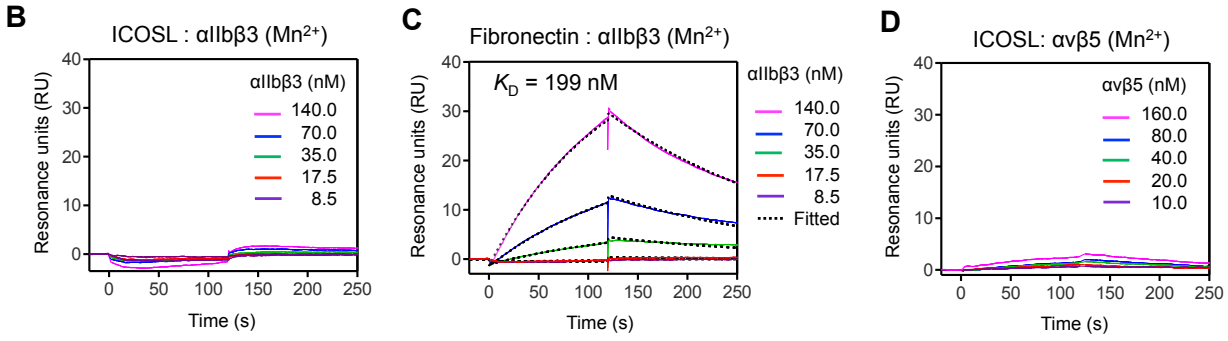

Supplemental Figure 6.

ICOSL selectively binds to αvβ3 but not to αIIbβ3 or αvβ5. (**A**) Table showing the binding characteristics of human ICOSL protein towards three different RGD-dependent integrins. N.B, no binding. (**B-D**) Representative sensorgrams depicting interaction of αIIbβ3 integrin with ICOSL (**B**) or fibronectin (**C**; positive control), and between αvβ5 and ICOSL (**D**) at various concentrations of integrins (0-140 or 0-160 nM in running buffer containing 2 mM Mn^{2+}). The average K_D values were determined from three independent experiments. Kinetic constants (k_a, k_d) were derived from locally fitting the association and dissociation phases using a 1:1 Langmuir binding model (black fitting curves) and affinities were calculated as $K_D=k_d/k_a$.

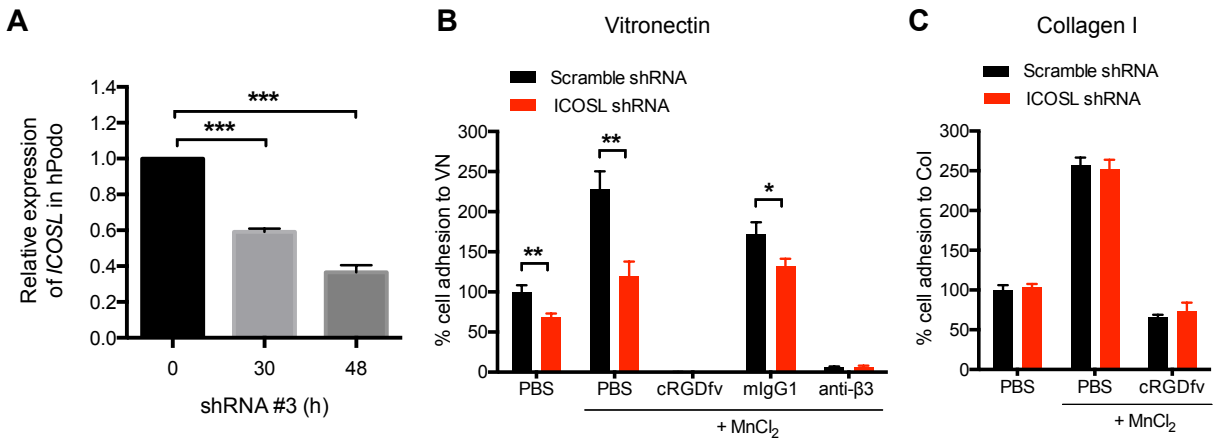

Supplemental Figure 7.

Knockdown of ICOSL inhibits β3 integrin-dependent podocyte adhesion. (**A**) *ICOSL* mRNA expression is reduced in human podocytes after treatment with shRNA-expressing lentivirus. Human podocyte cell lines were infected with a shRNA-scrambled control or shRNA-*ICOSL* #3 (selected among 4 shRNAs targeting ICOSL) lenti-virus. Twenty four hours after transduction, the cells were replaced with regular growth media and incubated for 30 to 48 hours. The level of *ICOSL* mRNA was determined by qPCR. Data are normalized to *GAPDH* expression (n=3 biological replicates). Data are mean±SD; ***P<0.001; One-way ANOVA with Tukey's multiple comparison test. (**B** and **C**) Loss of ICOSL function on human cultured podocytes measured by cell adhesion assay. Red bars represent adhesion levels of cells that were treated with shRNA targeting *ICOSL* while black bars represent levels from cells treated with a scrambled shRNA. Quantification of cell adhesion shows significantly reduced levels after treatment with shRNA targeting *ICOSL* on vitronectin-coated plates. The involvement of ICOSL was observed in the binding of cells in an RGD-dependent integrin manner when cells were plated on vitronectin (**B**), but not when plated on collagen I (**C**). Controls for this assay included the use of a competing peptide (cRGDfv) and an antibody directed against β3 integrin (or $mIgG_1$ as an isotype control) in combination with an integrin activator, $MnCl_2$. Data are shown as mean±SEM and from three independent experiments; *P<0.05, **P<0.01; One-way ANOVA with Tukey's multiple comparison test.

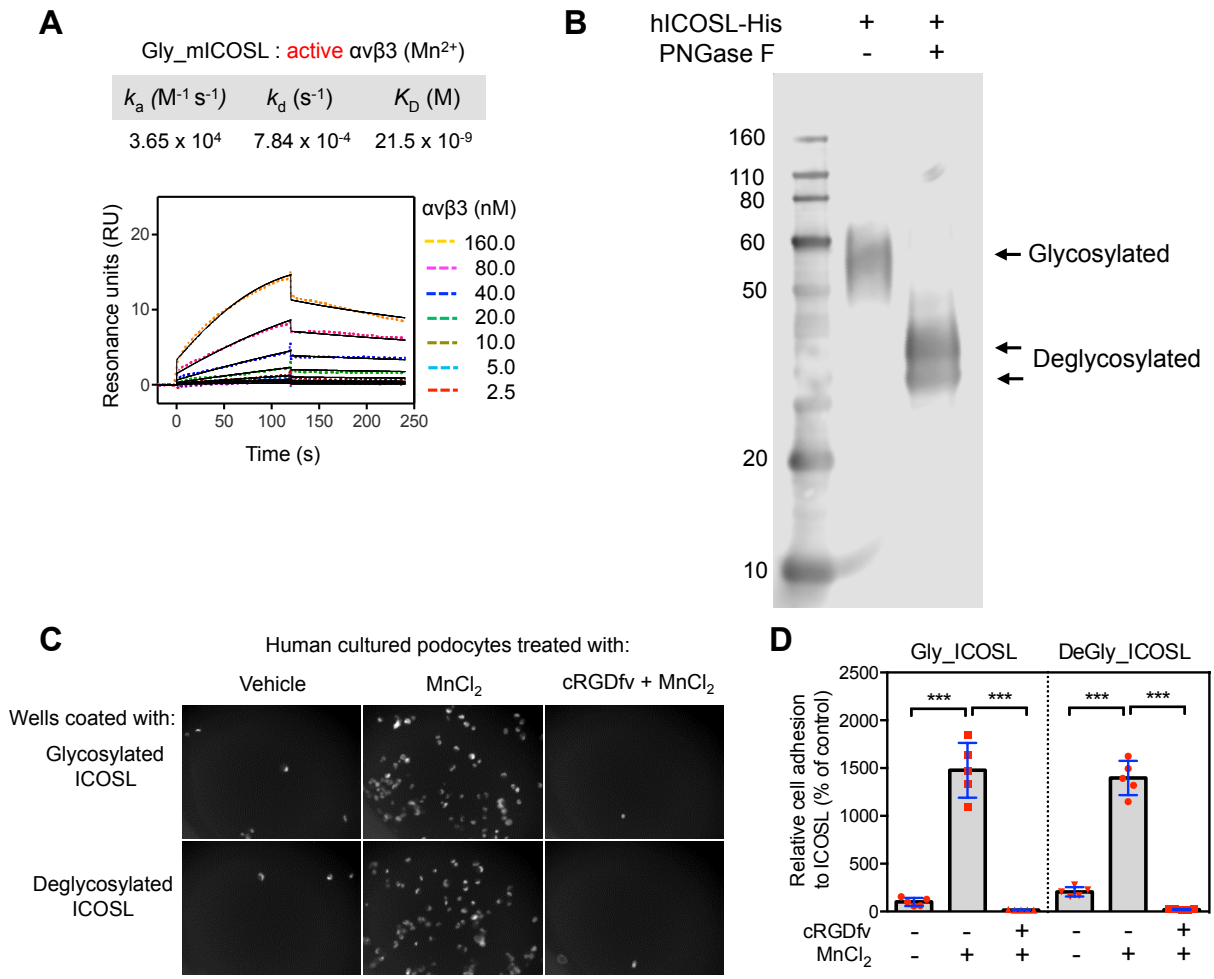

Supplemental Figure 8.

Glycosylation of ICOSL does not affect its ability to bind active αvβ3 integrin. (**A**) SPR kinetics analysis determined the equilibrium dissociation constant (K_D=21.5 nM) between immobilized glycosylated mouse ICOSL and αvβ3 integrin at various concentrations (0-160 nM). Kinetic constants (k_a, k_d) were determined by using a 1:1 Langmuir binding model (black fitting curves) and affinities were calculated as $K_D=k_d/k_a$. (**B**) PNGaseF treatment was performed following the manufacturer's protocol to deglycosylate human ICOSL-His protein (Thermo Scientific), followed by immunoblot analysis of the glycosylated and deglycosylated forms of the ICOSL protein using anti-His antibodies. Protein bands were visualized by the Odyssey imaging system. (**C**) Adhesion assay using cultured human podocytes. (**D**) Quantification of these adhesion assays (see Methods for details on the assay and how quantification was carried out). Data are mean±SD and from two independent experiments; **P*<0.05, ***P*<0.01, ****P*<0.001; One-way ANOVA with Tukey's multiple comparison test (**D**).

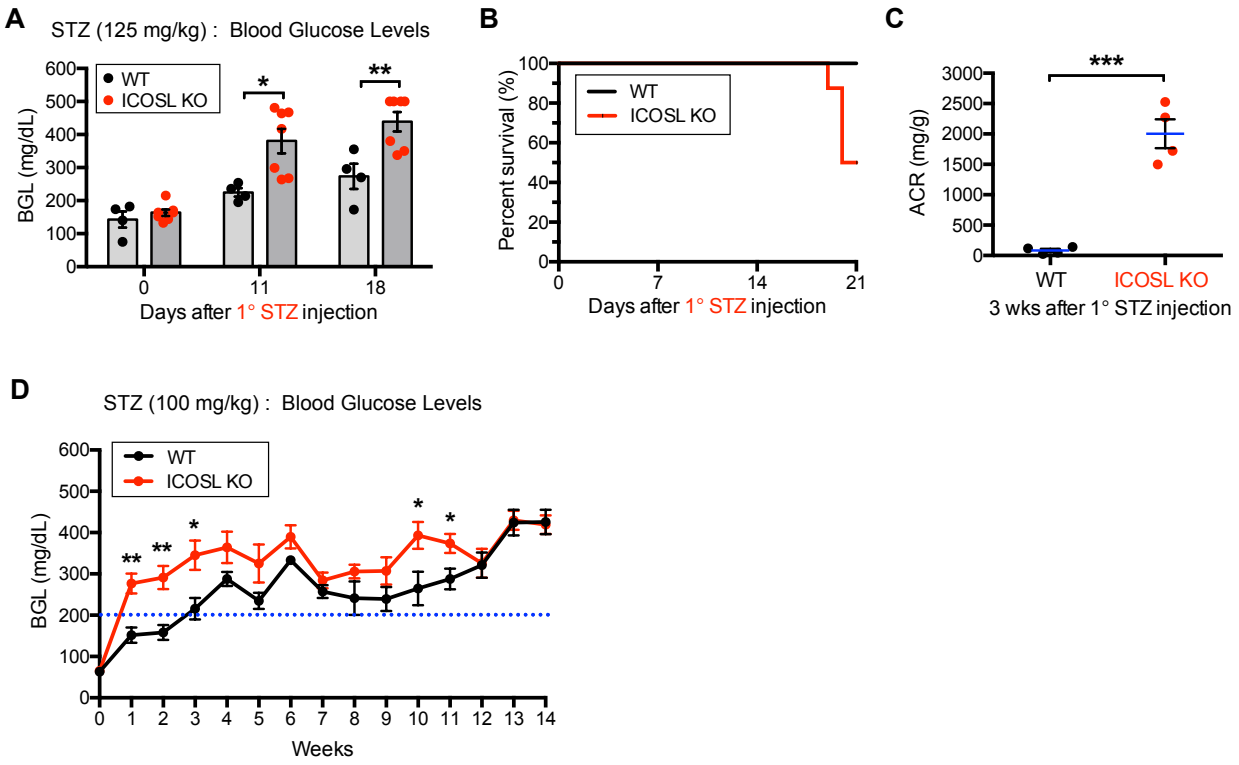

Supplemental Figure 9.

ICOSL deficient mice are more susceptible to the toxicity of STZ (125 mg/kg). (**A-C**) Diabetic ICOSL KO mice rapidly developed higher levels of hyperglycemia as compared to the WT mice (n=4–8 per group). (**A**) Eleven and 18 days after STZ treatment (125 mg/kg), the levels of hyperglycemia in ICOSL KO were significantly increased. (**B**) Survival rate was monitored for 21 days post STZ injection. (**C**) Albumin-to-creatinine ratio (ACR, mg/g) was calculated for surviving STZ-injected mice 21 days post injection. (**D**) Both BALB/c WT (black dots) and ICOSL KO (red dots) mice developed hyperglycemia by low dose STZ injection (100 mg/kg) (n=5–6 per group). The diabetic ICOSL KO mice rapidly developed higher levels of hyperglycemia as compared to WT mice. Three weeks after STZ treatment, the levels of hyperglycemia in either strain were sustained until 14 weeks. Data are mean±SEM; *P<0.05, **P<0.01, ***P<0.001; Multiple unpaired t test with the Holm-Sidak comparisons test (**A**, **D**); Student's two-tailed, unpaired t test (**C**).

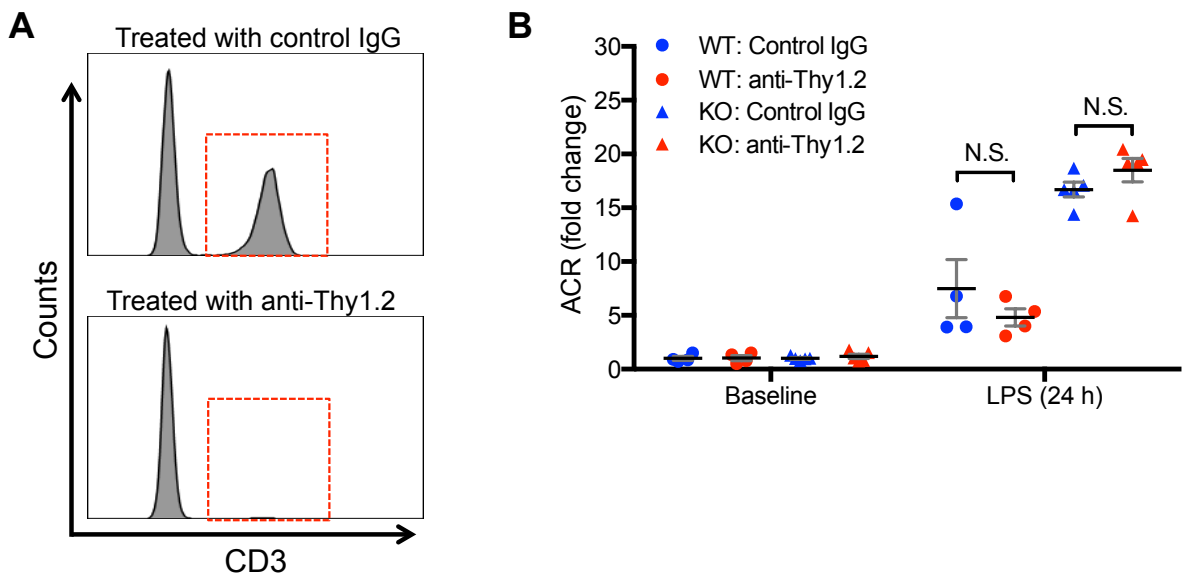

Supplemental Figure 10.

The renoprotective effect of ICOSL is not likely ICOS-dependent. Both WT and ICOSL KO mice were intravenously injected with monoclonal antibody against Thy1.2 (5 mg/kg) or rat IgG2a (5 mg/kg) 24 hours prior to LPS injection (2.5 mg/kg, i.p) (n=4 for WT+control IgG and WT+anti-Thy1.2, n=5 for KO+control IgG and KO+anti-Thy1.2). Urine and blood samples were collected at baseline and 24 hours after LPS treatment. Blood leukocytes were labeled with fluorescently conjugated antibodies specific for mouse CD3. (**A**) Representative histogram of flow cytometric analysis showing T cell depletion in mice treated with anti-mouse Thy1.2. (**B**) Albumin/creatinine (ACR) levels in WT and ICOSL KO mice treated with either control IgG or anti-Thy1.2. ACR levels normalized to baseline are shown as fold change. There was no statistically significant difference in ACR levels between T cell-depleted and control groups in both WT and KO mice. Data are mean±SEM; N.S., not significant; Two-way ANOVA with Tukey's multiple comparison test.

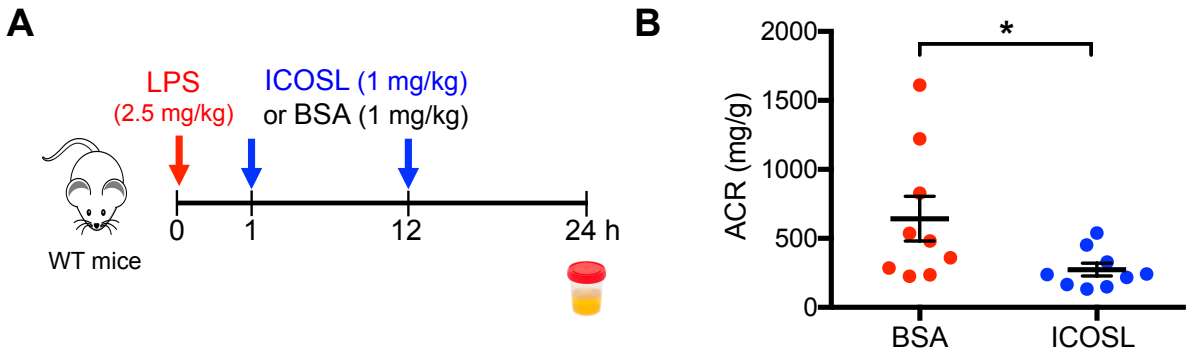

Supplemental Figure 11.

Administration of ICOSL WT reduces proteinuria in LPS-injected WT mice. BALB/c WT mice were challenged with 2.5 mg/kg LPS, then intravenously injected with mouse ICOSL protein (1 mg/kg) or BSA (1 mg/kg) as a protein control 1 and 12 hours after LPS injection. Urine samples were collected before injection then 12 and 24 hours after LPS administration. Schematic representation of the experimental design (**A**) and ACR levels (**B**) in WT mice injected with either ICOSL protein (blue dots) or BSA (red dots) 24 hours after LPS injection (n=9 per group from two independent experiments). Data are mean±SEM; *P<0.05; Student's two-tailed, unpaired t test (B).

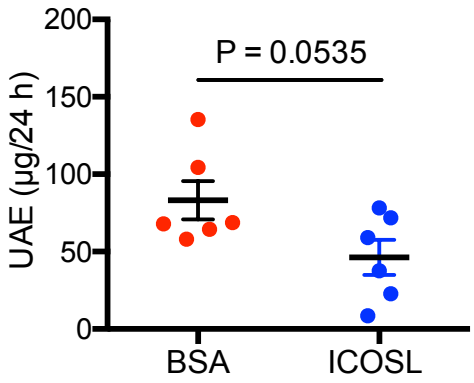

Supplemental Figure 12.

ICOSL treatment had a trend toward lower proteinuria in STZ-induced DN mice.

Urinary albumin excretion (UAE) for 24 hours in ICOSL KO mice treated with either ICOSL protein (blue dots) or BSA (red dots) (n=6 per group from one experiment). In brief, male ICOSL KO mice were challenged with STZ to induce diabetes. Two weeks after STZ injection, the mice were divided into 2 groups. Each group (n=6/group) was treated with either mouse ICOSL protein (1 mg/kg, i.p, twice/week) or BSA as a protein control for 4 weeks. For the measurement of urinary albumin excretion, urine samples were collected using metabolic cages at 6 weeks after STZ administration (ICOSL/BSA treatment for 4 weeks). Data are mean±SEM; Student's two-tailed, unpaired t test.

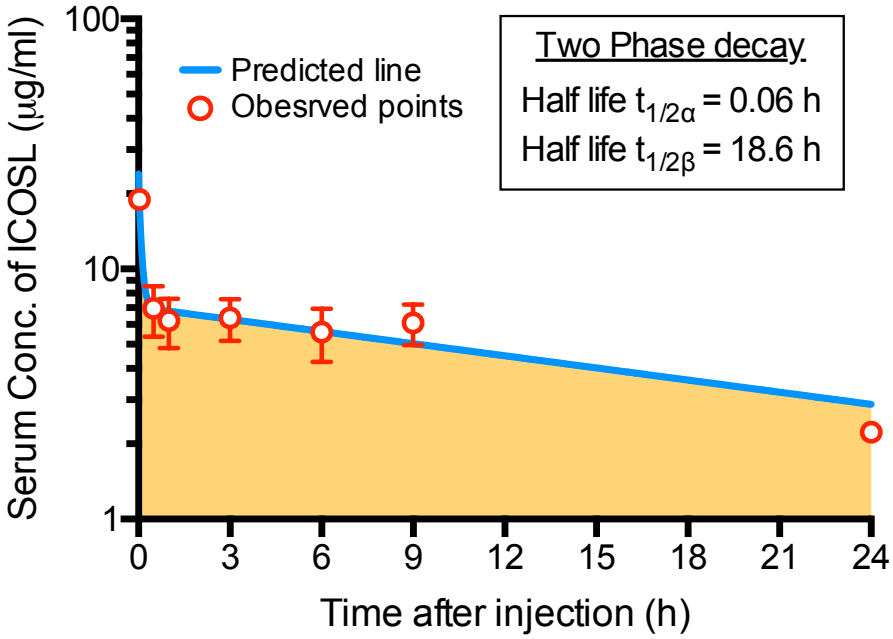

Supplemental Figure 13.

The pharmacokinetic (PK) study of ICOSL in mice. *Icosl* KO mice (12-week old female, n=3) were intravenously injected with ICOSL-AF488 conjugate (1 mg/kg body weight). Blood samples (about 30-40 μl) were collected from the retro-orbital plexus at 0.03, 0.5, 1, 3, 6, 9, and 24 hours following ICOSL administration. After spinning down the blood samples at 13,000 rpm for 5 min, sera were obtained and diluted 10-fold with PBS. Standard curve (ranging from 0.156 to 10 μg/ml) was prepared by using serial dilution of the injected ICOSL-AF488 conjugate with PBS containing 10% (v/v) control mouse serum. Fluorescence intensities of standards and diluted sera were measured at 485 nm excitation and 528 nm emission using a fluorescence plate reader (BioTek). The data at each time point were displayed as mean ± SEM and fitted to the equation for two phase decay using Prism version 6.0 (GraphPad).

References

1. Sievers F, Wilm A, Dineen D, Gibson TJ, Karplus K, Li W, Lopez R, McWilliam H, Remmert M, Soding J, et al. Fast, scalable generation of high-quality protein multiple sequence alignments using Clustal Omega. *Mol Syst Biol.* 2011;7(539).